

22. A COMPARATIVE STUDY OF FATIGUE CRACK RETARDATION  
IN AIR AND VACUUM

N. RANGANATHAN, J. PETIT and A. NADEAU  
Laboratoire de Mécanique et de Physique des Matériaux  
E.N.S.M.A. Rue Guillaume VII - 86034 POITIERS CEDEX  
E.R.A. - C.N.R.S. n° 123

INTRODUCTION.

The sensitivity of fatigue crack growth phenomena to varying loads has been a subject of interest and importance. In one of his earliest studies, SCHIJVE (1) had elucidated the retarding effect of a spike type overload on a pre-grown crack at constant amplitude. Since then a number of researchers have contributed to the understanding of this delay phenomenon and most of the physical and mechanical factors governing it have been defined (2,3).

To get a new insight into this problem, we have chosen vacuum as the environment which, at constant amplitude tests leads to much lower growth rates (4). This paper presents the results obtained in a series of comparative overload tests in air and vacuum.

EXPERIMENTAL CONDITIONS.

The tests were carried out on 10 mm thick CT75 specimens of 2024-T 351, Aluminium alloy. The machine used was an Instron electro-hydraulic testing machine of 2500 daN capacity. The vacuum tests were carried out in an environmental chamber in which a vacuum of  $10^{-3}$  Pa or less could be obtained.

All tests were done at a constant base load amplitude,  $\Delta P_i$  of 600 daN. Two load ratios  $R = 0.01$  and  $R = 0.1$  were considered. The overload ratio, defined by  $\Delta K_{peak}/\Delta K_i$  was 2.0 for all tests. The test frequencies were 5 Hz for tests in air and 35 Hz in vacuum while the overloads were applied at 0.2 or 0.02 Hz. The crack growth on the polished surface was observed through a travelling microscope.

The plastic zone sizes were determined by the optical interferential method of NOMARSKI. Fractographic studies were carried out in a JEOL JSM 50A - electron microscope.

EXPERIMENTAL RESULTS AND INTERPRETATION.

1) Crack propagation behaviour.

Figure 1 shows the evolution of the crack length  $a$ , with the number of cycles  $N$ , following an overload in the two environments considered. The experimental conditions were :

$$\Delta K_I = 15.7 \text{ MPa}\sqrt{\text{m}}, \text{ for both air and vacuum}$$

$$R = 0.1$$

overload frequency = 0.02 Hz.

Immediately following the overload, there is a small acceleration of the crack, following which the crack progressively retards as indicated by the minimal change in "a" with respect to  $N$  and finally the crack accelerates again as indicated by the change in curvature of the curves.

The number of delay cycles  $N_d$ , is defined as the number of cycles required from the point of application of the overload up to the point where the crack regains its initial growth rate, existing before the application of the overload (fig. 1).

The associated crack length is defined as the overload affected crack length  $a_d$ .

Figure 2 gives the relationship between  $N_d$  and  $\Delta K_{\text{peak}}$ . One can see that  $N_d$  values increase with  $\Delta K_{\text{peak}}$  in air and vacuum and that  $N_d$  values in vacuum are much greater than those in air. For the same  $\Delta K_{\text{peak}}$ ,  $N_d$  in vacuum can be 5 to 10 times larger than that in air.

Figure 3 shows the variation of  $\frac{da}{dN}$  with  $a$  for the same tests, as in figure 1. One can see that :

- The initial propagation rate,  $(\frac{da}{dN})_i$  in vacuum is a bit smaller.
- The minimal growth rate  $(\frac{da}{dN})_{\text{mini}}$  is much smaller in vacuum.
- $a_d$  in vacuum is greater than that in air and the difference is more evident after  $(\frac{da}{dN})_{\text{mini}}$  i.e. during the acceleration phase. Figure 4 indicates the relationship between  $K_{\text{peak}}$  and  $a_d$  for the present series of tests. It is evident that at higher values of  $K_{\text{peak}}$ ,  $a_d$  values in vacuum can be 1.5 times larger than those in air.

Plastic Zone.

Earlier researches (5) had attempted to relate  $a_d$  with

the plastic zone created by the overload. Figure 4 compares  $a_d$  values with the diameter of the plastic zone given by the IRWIN model (6) :

$$2r_y = \frac{1}{\pi} \left( \frac{K_{\text{peak}}}{\sigma_{ys}} \right)^2$$

and figure 5 gives the scatter in the plastic zone sizes measured in comparison with the IRWIN model.

From these two figures we can derive that :

- Plastic zone sizes in vacuum are larger than those in air which confirms BOUCHET 's results (7).
- A similar trend is observed in the evolution of the  $a_d$  values.
- Experimentally observed  $2r_y$  are smaller than  $a_d$  at higher values of  $K_{\text{peak}}$ .

In both the environments the observed plastic zones are in the form of wings the angle between which is more acute in air (fig. 6).

In all tests we have been able to observe a zone of very little deformation between these wings and near the plane of the crack where the crack progressively retards after the overload (fig. 6). Subsequently in the region where the crack starts accelerating, we have been able to locate the point of reappearance of the plastic zone. We have defined the corresponding crack length as  $a^*$ .

Initial observations (8) showed that  $a^*$  may be related to the crack length to attain  $\frac{da}{dN}_{\text{mini}}$  defined as  $a_r$  in figure 3). Figure 7 shows the relation between these two parameters and  $\Delta K_{\text{peak}}$ . One can observe that  $a^*$  is systematically greater than  $a_r$ . One can also see that  $a^*$  and  $a_r$  have a similar evolution in the two environments studied. We consider that observed  $a^*$  values are greater than  $a_r$  because the optical method used is not accurate enough to detect very small plastic zone sizes and hence the exact beginning of its reappearance.

Macroscopic appearance of the fracture surface.

Macroscopically the overload, at low  $K_{\text{peak}}$ , is characterised by a dark thin band in vacuum as well as in air (fig. 8). The thickness of this band increases with increasing  $K_{\text{peak}}$ . The fracture surface in vacuum is lighter due to the absence of oxidation.

The evolution of the tear size at the centre of the specimen with  $K_{\text{peak}}$  leads to an interesting result (Fig. 9). As can be seen here, the tear size in vacuum is clearly larger than that in air. This difference can be as high as 50% for the same value of  $K_{\text{peak}}$  and apparently it is independent of the frequency in the range considered.

Microscopic appearance of the fracture surface.

Microscopically, in air, the overload is characterised by the formation of a stretch band. The fractographic features following this stretch band depends upon the intensity of the overload. With increasing  $K_{peak}$  one finds either poorly formed striations or striations and dimples or just dimples following this band (5).

Apparently a similar feature was found in vacuum : fig. 10 gives comparative fractographs in the two environments, even though striations are not clearly discernible in vacuum. In fact, the periodic spacing which we could observe in the direction of crack propagation appeared to be unrelated to the macroscopic growth rate and were attributed to coarse slip. This is in agreement with the observations found elsewhere (9).

We found comparative fractographic features before the overload and at a distance approximately equal to  $a_d$  from it (8). The evolution of the fracture surfaces, along the crack front showed that after a strong overload the crack reached its initial velocity for a shorter crack growth at the centre of the specimen than near the edges. This is in agreement with the observations of BATHIAS for tests in air (3).

Discussions.

The present series of tests have shown that qualitatively the effect of an overload in vacuum is essentially similar to that in air. In fact, we have observed a similar evolution of  $a_d$ ,  $N_d$ ,  $(\frac{da}{dn})_{min}$  etc with respect to  $\Delta K_{peak}$  and  $\Delta K_i$  in both the environments, at constant value of overload ratio.

Earlier analysis suggested that the distribution of residual stresses following the overload are apparently similar in the two environments and the quantitative differences otherwise observed should be related to the inherent differences in the material behaviour (8). Thus it has been shown in Réf. 8 that the retarded growth rate  $\frac{da}{dn}_{min}$  leads to the same  $\Delta K$  values based on crack propagation curves near the threshold (4).

The apparent absence of discernible plastic deformation near the plane of the crack after the overload upto the point of crack acceleration leads up to conjecture on the possible mechanism of retardation.

A strong overload tends to cause brittle fracture at the centre of the specimen as is manifest in the crescent shaped tear. Following this, for overloads not causing crack arrest, the crack propagates only in the two ligaments near the surfaces upto the point of crack acceleration as has been shown before (3). In fact, in exploratory tests causing crack arrest in vacuum (overload ratios = 2.3) we have observed that the crack grew very slowly near the surfaces upto 6 million cycles after the overload even

though subsequent fractographic analysis showed that the crack remained blocked at the centre.

In this region where the crack grows slowly near the surfaces to regain its curvature, the crack growth is not accompanied by plastic zone formation near the crack plane as has been shown presently. A definition of the conditions of crack growth in this phase should involve a three dimensional analysis of the stress distribution following the overload, the local material hardening and the crack front modification. Apparently it is not a simple task.

Once the plastic zone is re-formed, it increases in size until the crack reaches its non-retarded growth rate (fig. 6). For a plastic zone size optically determined in this phase we have calculated the value of  $\Delta K$  based on RICE's model (10) : the crack propagation rate for this  $\Delta K$  from the data near threshold for this material (4) compare well with the rate observed experimentally - Fig. 11 gives a typical example of this analysis.

The difference in tear sizes observed in vacuum and air can be explained by a stronger plastification in vacuum as shown by BOUCHET (7) and confirmed by our results. A stronger plastification means a larger plastic zone, more work-hardened ; thus the possibility of brittle fracture is enhanced in vacuum.

Conclusions.

This series of tests to compare the fatigue crack retardation phenomena following a single overload in air and vacuum leads us to the following conclusions :

- 1) Qualitatively the effect of an overload in these two environments is essentially the same and the quantitative differences could be related to the inherent differences in fatigue crack behaviour in the two environments.
- 2) A retardation model in vacuum can be proposed which is comparable to the one proposed by BATHIAS (3) for the delay process in air. In other words :
  - a) A strong overload is accompanied by a tear in the plane strain region. The related crack growth near the surfaces is small : thus the crack front curvature is changed.
  - b) The crack is practically blocked at the centre of the specimen while there is crack propagation at a decreasing rate in the two ligaments near the surfaces as the crack front tends to regain its initial curvature. The present tests have shown that this phase is accompanied by no perceptible plastic zone formation in the surfaces.

c) Once the crack front curvature reaches its initial value before the overload, the crack accelerates back to attain its nonretarded growth rate. In this zone for a given growth rate, the observed plastic zone sizes leads to values of  $\Delta K$  (based on RICE's model) which correspond to a comparable growth rate on the basis of crack propagation curves without overloads.

Acknowledgment.

The authors wish to acknowledge the "Délégation Générale à la Recherche Scientifique et Technique" for giving financial support for this work by their contract n° 650-21.

Références.

- 1) J. SCHIJVE, D. BROEK and P. RIJK,  
Nat. Aero. Lab. NLR MP 2094 (1961).
- 2) D.M. CORBLI and P.F. PACKMAN,  
Eng. Frac Mech. 5 (1973) p. 479.
- 3) C. BATHIAS and M. VANCON,  
Eng. Frac. Mech. 10, 2 (1978) p. 409.
- 4) J. PETIT, B. BOUCHET, C. GASC and J. de FOUQUET,  
ICF4, Waterloo Canada, Fracture 1977 vol. 2, p. 867.
- 5) E.F.J. VON EUW, R.W. HERTZBERG and Richard ROBERTS,  
ASTM STP 513 (1972) p. 230.
- 6) F.A. Mc. CLINTOCK and G.R. IRWIN,  
ASTM STP 381 (1965) p. 84.
- 7) B. BOUCHET, J. de FOUQUET et M. AGUILLON,  
Acta Met. 13 (1975) p. 1325.
- 8) N. RANGANATHAN, J. PETIT and B. BOUCHET,  
Eng. Frac. Mech. (To be published).
- 9) D. BROEK,  
Engg. Frac. Mech. 1, (1970) p. 691.
- 10) J.R. RICE,  
ASTM STP 415 (1967) p. 247.

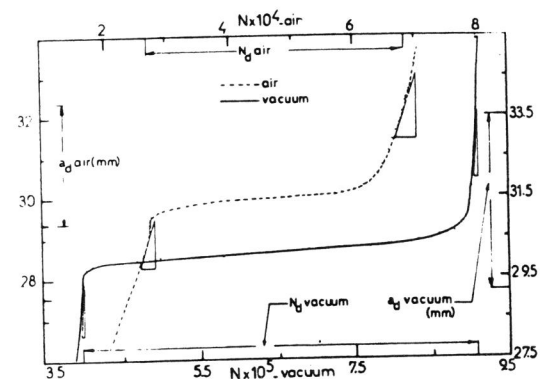


Figure 1 : Comparative evolution of a with N in air and vacuum following an overload.

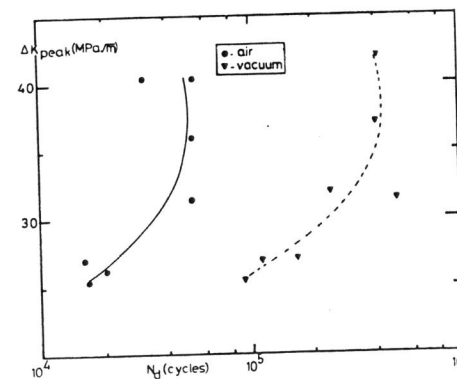


Figure 2 : Evolution of  $N_d$  with  $\Delta K_{peak}$  in the two environments.

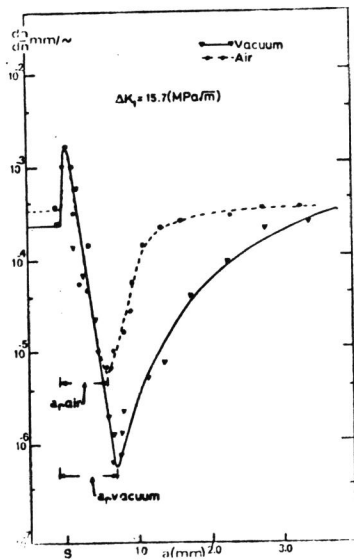


Figure 3 :  $\frac{da}{dN}$  vs  $a$  curves following an overload in air and vacuum.

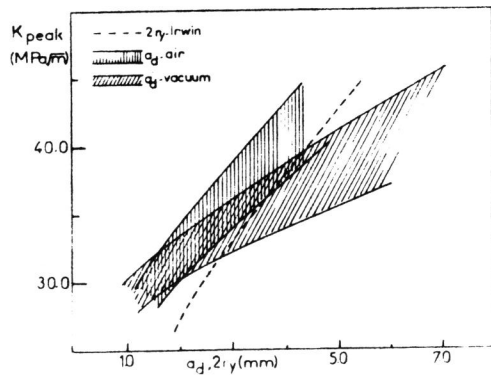


Figure 4 : Relationship between overload affected crack length and plastic zone size given by the IRWIN model.

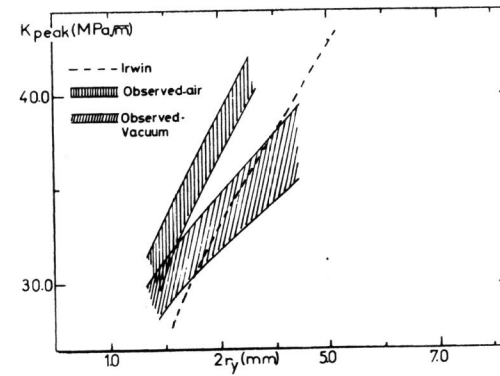


Figure 5 : Scatter in plastic zone sizes experimentally obtained compared with the IRWIN model.

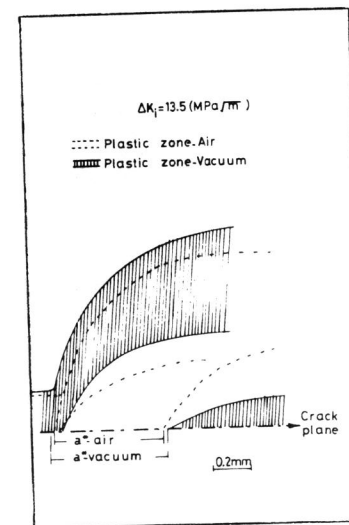


Figure 6 : Schematic evolution of the plastic zone : air and vacuum.

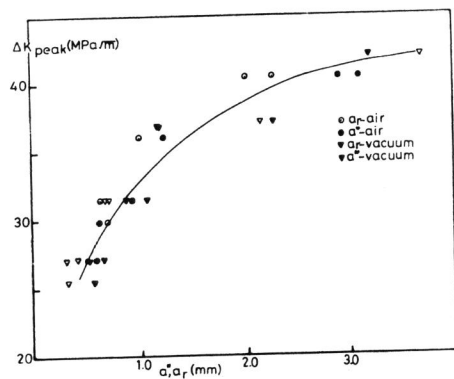


Figure 7 : Relationship between  $a^*$  and  $a_r$ .

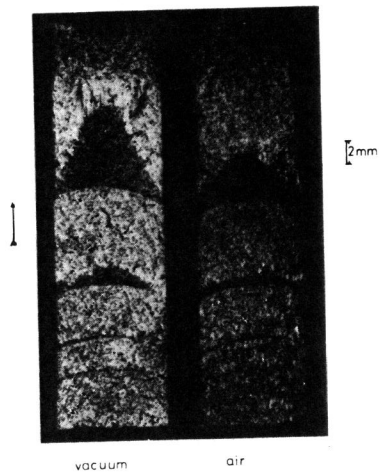


Figure 8 : Macroscopic appearance of the fracture surfaces.

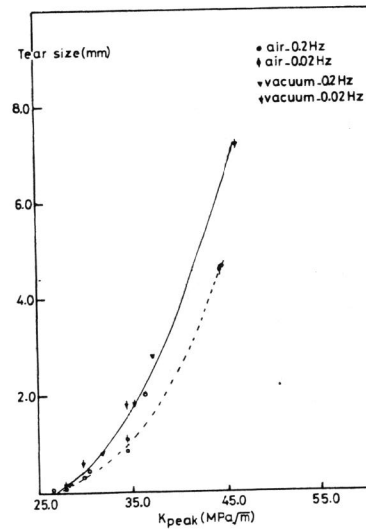


Figure 9 : Evolution of the tear size with overload intensity.

$\Delta K_{peak} = 31.4 (MPa\sqrt{m})_{air}$

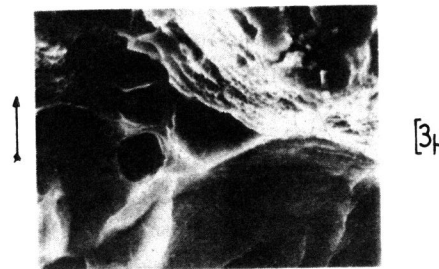


Fig. 10 (a).

Figure 10: Comparative fractographs due to an overload in the two environments.

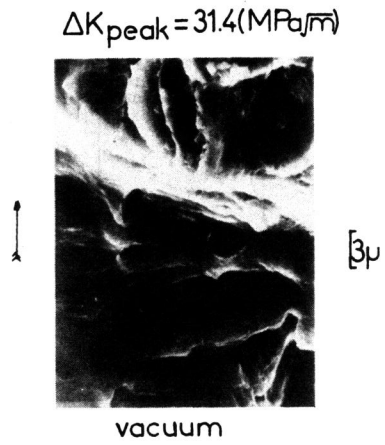


Fig. 10 b.

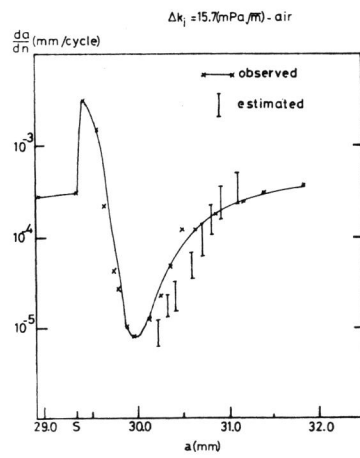


Figure 11: Crack growth rates based on plastic zone size evolution in the acceleration phase compared with observed values.